Learning-Based Entanglement Detection in Two-Qubit Systems Using Partial Pauli Expectation Values

Ameema Tahir, Jae Uk Roh, and Hyundong Shin
Department of Electronics and Information Convergence Engineering, Kyung Hee University, Republic of Korea
Email: hshin@khu.ac.kr

***Abstract*—Quantum entanglement lies at the heart of many quantum information protocols, yet detecting it often requires full tomography—a resource-intensive process. In this work, we develop and analyze a machine-learning approach that classifies entanglement in two-qubit states using only a limited subset of Pauli measurements. Our approach leverages a feedforward neural network, trained on two large synthetic datasets: one comprising only pure states and another consisting of pure and mixed states. We systematically investigate how classification accuracy changes with the number of measured observables, comparing cases in which we measure 3, 5, 7, or 9 different tensor-product Pauli operators. Ground-truth labels are assigned via concurrence, a well-established measure of two-qubit entanglement. Our results demonstrate that increasing the number of observables leads to higher classification accuracy, with a peak of 99% for pure states and 97% for mixed states when using nine observables. These findings underscore the capacity of partial measurement schemes, coupled with neural networks, to reduce measurement overhead in near-term quantum experiments.**

***Index Terms*—Quantum entanglement, two-qubit states, machine learning, neural networks, partial measurements, quantum state characterization, concurrence, Pauli operators.**

I. Introduction

Entanglement is a fundamental resource that distinguishes quantum mechanics from classical physics and underpins many quantum information tasks, such as quantum teleportation, superdense coding, and quantum key distribution [1]. Efficiently distinguishing separable from entangled states [2], [3] is therefore critical for both theoretical investigations and practical applications. Traditionally, one might perform full state tomography, reconstructing the density matrix from complete measurement data. However, as the system size grows, quantum tomography becomes prohibitively expensive, scaling exponentially with the number of qubits.

This work addresses a crucial question: Can we reliably detect two-qubit entanglement by measuring fewer observables than are required for full tomography? Specifically, we propose a machine-learning (ML) framework [4], [5] that takes as input a small subset of Pauli measurement outcomes i.e. just 3, 5, 7, or 9 tensor-product Pauli operators and predicts whether a two-qubit state is entangled or separable. We thoroughly assess the performance of a feedforward neural network on two large datasets: one composed solely of pure states and one containing both pure and mixed states. We label states using the concurrence criterion, thus providing consistent ground-truth measures of entanglement [6].

This paper improves upon existing studies in several ways:

- **Systematic Variation of Measurement Operators:** We explore four distinct subsets of Pauli operators, quantifying the trade-off between measurement overhead and classification accuracy.
- **Comprehensive Dataset Generation:** We generate 100,000 states in each scenario (pure and mixed), ensuring broad coverage of separable and entangled states. Importantly, the mixed-state dataset includes both convex mixtures of product states and entangled states from the Ginibre ensemble, ensuring diverse and well-separated examples.
- **Novelty in Partial-Measurement ML:** By focusing on a minimal yet strategically chosen set of Pauli measurements, we showcase how partial measurement data can suffice to accurately detect entanglement. Our findings underscore the feasibility of implementing resource-efficient witness schemes in near-term quantum platforms.

In the following Section II, we introduce the theoretical background of concurrence and partial measurement. We then detail how we generate and label the states, specifying pure vs. mixed-state datasets in Section III. Afterward, we describe our neural network model and training procedure in Section IV. The results are presented and discussed in Section V, including a thorough comparison of different measurement sets and a justification of the measured improvement. Finally, we conclude with potential extensions and practical implications in Section VI.

II. Theoretical Background

A. Two-Qubit Entanglement and Concurrence

For a general two-qubit state ρ, a standard measure of entanglement is the concurrence, $C(\rho)$. In the special case of a pure two-qubit state $|\psi\rangle$, concurrence is defined by

$$C(|\psi\rangle) = |\ \langle\psi^*|(\sigma_y \otimes \sigma_y)|\psi\rangle\ |, \tag{1}$$

where $|\psi^*\rangle$ denotes the complex conjugate of $|\psi\rangle$ in the computational basis, and σ_y is the Pauli Y operator. A pure two-qubit state is separable if and only if its concurrence is zero.

For mixed states, one computes $C(\rho)$ by first determining the eigenvalues of the non-Hermitian matrix $R = \rho(\sigma_y \otimes \sigma_y)\rho^*(\sigma_y \otimes \sigma_y)$. Let $\lambda_1, \lambda_2, \lambda_3, \lambda_4$ be the square roots of the eigenvalues of the positive semi-definite matrix R, sorted in descending order ($\lambda_1 \geq \lambda_2 \geq \lambda_3 \geq \lambda_4$). The concurrence of ρ is then given by the standard Wootters formula [6]:

$$C(\rho) = \max\{0, \lambda_1 - \lambda_2 - \lambda_3 - \lambda_4\}, \tag{2}$$

A two-qubit state is entangled if and only if $C(\rho) > 0$. Here, we apply a practical buffer zone on the value of $C(\rho)$ to account for numerical round-off, defined in section III.

B. Partial Measurements with Tensor-Product Pauli Operators

Full quantum state tomography of a two-qubit system requires measurements in multiple bases to reconstruct all 16 density-matrix elements. In contrast, we consider smaller sets of tensor-product Pauli operators. The standard single-qubit Pauli matrices are

$$\sigma_x = \begin{pmatrix} 0 & 1 \\ 1 & 0 \end{pmatrix}, \quad \sigma_y = \begin{pmatrix} 0 & -i \\ i & 0 \end{pmatrix}, \quad \sigma_z = \begin{pmatrix} 1 & 0 \\ 0 & -1 \end{pmatrix}, \tag{3}$$

We define, in Table I, four fixed subsets of tensor-product Pauli operators. Each subset $\mathcal{O}_k$ contains k observables, where $k \in \{3, 5, 7, \ \}$. For every two-qubit state ρ (or $|\psi\rangle$ in the pure-state case), we record the real expectation value

$$\langle O \rangle = \mathrm{Tr}[\rho\, O], \quad \text{for } O \in \mathcal{O}_k \tag{4}$$

which yields a k-dimensional real feature vector forming the input vector for our machine learning classifier.

TABLE I
EXACT TENSOR-PRODUCT PAULI OPERATOR SUBSETS

k	$\mathcal{O}_k$
3	$\{\sigma_x \otimes \sigma_x,\ \sigma_y \otimes \sigma_y,\ \sigma_z \otimes \sigma_z\}$
5	$\mathcal{O}_3 \cup \{\sigma_x \otimes \sigma_y,\ \sigma_y \otimes \sigma_x\}$
7	$\mathcal{O}_5 \cup \{\sigma_x \otimes \sigma_z,\ \sigma_z \otimes \sigma_x\}$
9	$\mathcal{O}_7 \cup \{\sigma_y \otimes \sigma_z,\ \sigma_z \otimes \sigma_y\}$

III. Dataset Generation

We produce two separate datasets, each of size $N = 100,000$. One dataset comprises pure two-qubit states, while the other contains a balanced mix of pure and mixed states. In both datasets, 50% of the states are labeled "separable" and 50% labeled "entangled".

A. Pure-State Dataset

All pure two-qubit states are sampled from the uniform (Haar) measure on $\mathbb{C}^4$. Their concurrence is evaluated as given by (1).

States with

$$C\big(|\psi\rangle\big) < 10^{-9}$$

are labeled **separable**, while those with

$$C\big(|\psi\rangle\big) > 10^{-7}$$

are labeled **entangled**. Candidates falling into the buffer zone $10^{-9} \leq C \leq 10^{-7}$ are discarded. Sampling continues until $N_{\text{pure}} = 100{,}000$ states (balanced 50–50 between classes) are obtained.

B. Mixed-State Dataset

For mixed states we again target a 50–50 class balance with a concurrence buffer around zero.

Separable mixed states: Each separable density matrix is generated as a generic convex mixture of product states:

$$\rho_{\text{sep}} = \sum_{k=1}^{K} p_k \big(|\phi_k^{(A)}\rangle\langle\phi_k^{(A)}|\big) \otimes \big(|\phi_k^{(B)}\rangle\langle\phi_k^{(B)}|\big), \tag{5}$$

where $K \sim$ ni $\{2, 3, 4, 5\}$, the coefficient vector $(p_1, \ldots, p_K) \sim$ Diric le $(1, 1, \ldots)$, and each single-qubit pure state $|\phi_k^{(A/B)}\rangle$ is sampled uniformly from the Bloch sphere. Samples whose concurrence

$$C(\rho_{\text{sep}}) > 10^{-9}$$

are rejected and resampled.

Entangled mixed states: Entangled states are drawn from the Ginibre ensemble:

$$\rho = \frac{GG^\dagger}{\mathrm{Tr}[GG^\dagger]}, \tag{6}$$

with $G \in \mathbb{C}^{4\times4}$ having i.i.d. complex Gaussian entries. We accept samples satisfying

$$C(\rho) > 10^{-7},$$

discard those in the buffer zone $10^{-9} \leq C(\rho) \leq 10^{-7}$, and top up the entangled pool with a 10% quota of Werner-type mixtures:

$$\rho_{\text{Bell}}(\lambda) = (1-\lambda)|\ \ ^+\rangle\langle\ \ ^+| + \lambda\, \frac{\mathbb{1}}{4}, \qquad \lambda \sim \mathcal{U}[0, 0.2]. \tag{7}$$

Finally, the union of the separable and entangled pools is shuffled, ensuring no trivial order effects. The dataset is then split into training, validation, and test sets as described in following section.

IV. Machine Learning Framework

A. Neural Network Architecture

We employ a feedforward neural network implemented in TensorFlow. For each measurement subset (3, 5, 7, or 9 operators, denoted by k), the network input layer has dimension k. The architecture is:

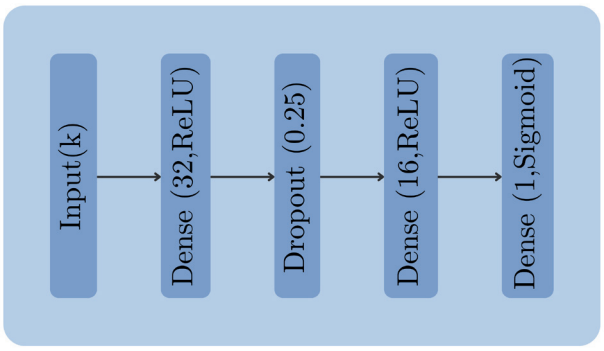

Fig. 1. Feedforward neural network architecture mapping k-dimensional Pauli inputs to binary entanglement output.

TABLE II
PURE-STATE MODEL PERFORMANCE FOR DIFFERENT NUMBERS OF OBSERVABLES

Obs	Test Acc.	Loss	Val Ep.	Val Loss	Val Acc.
3	75.13%	0.4672	156	0.4701	74.89%
5	88.98%	0.2633	175	0.2705	88.48%
7	93.98%	0.1656	136	0.1687	93.89%
9	99.16%	0.0422	150	0.0439	99.09%

TABLE III
MIXED-STATE MODEL PERFORMANCE FOR DIFFERENT NUMBERS OF OBSERVABLES

Obs	Test Acc.	Loss	Val Ep.	Val Loss	Val Acc.
3	68.24%	0.5730	91	0.5735	67.93%
5	87.12%	0.2614	38	0.2666	86.82%
7	94.14%	0.1232	78	0.1254	93.99%
9	97.58%	0.0618	118	0.0607	97.74%

where the final neuron outputs a probability $\hat{y} \in (0, 1)$ indicating the model's prediction of entanglement (1 for entangled, 0 for separable).

B. Training Procedure

We standardize each feature across the training set using a standard scaler. The data is split into 80% training and 20% testing, with 20% of the training set used for validation. Training is performed for up to 200 epochs using the Adam optimizer with a learning rate of 5×10^{-4}. We use a binary cross-entropy loss function. Early stopping is implemented, halting training if the validation loss does not improve for 25 consecutive epochs, and restoring the model weights from the epoch with the lowest validation loss. The batch size used during training is 64.

V. EXPERIMENTAL RESULTS

We present results for both the pure-state and mixed-state datasets. Each table below summarizes the performance on the test set, including accuracy and loss, along with details from the validation phase during training.

A. Pure States

Table II shows performance metrics on the pure-state dataset. Even with only 3 Pauli observables, the network achieves roughly 75% accuracy. Performance significantly improves as more observables are included. With 9 measured observables, accuracy reaches 99.16%, demonstrating that partial measurements can be highly effective for entanglement detection in pure states.

These high accuracies reflect that pure-state concurrence can often be inferred from a few key correlators (e.g., combinations involving $\sigma_x \otimes \sigma_x$, $\sigma_y \otimes \sigma_y$, $\sigma_z \otimes \sigma_z$). With a sufficiently rich measurement basis (like 9 operators), the network effectively learns the geometric separation between separable and entangled pure states.

B. Mixed States

Table III summarizes the performance on the more challenging mixed-state dataset. While accuracies are slightly lower than for pure states, especially with fewer observables, the trend of improvement with more measurements holds. Using 9 observables yields a high test accuracy of 97.58%, demonstrating the method's utility even for complex mixed states.

The significant accuracy increase from 3 to 9 observables highlights the necessity of richer measurement data for mixed states, where entanglement can be hidden in subtle correlations and off-diagonal density matrix elements that require multiple complementary measurement settings to probe effectively.

VI. CONCLUSION AND OUTLOOK

We have demonstrated a machine-learning approach for detecting entanglement in two-qubit states using only partial measurement data from 3, 5, 7, or 9 tensor-product Pauli observables. Trained on large synthetic datasets, a simple feed-forward neural network achieved high classification accuracy: over 99% for pure states and nearly 98% for mixed states when provided with 9 observables.

These results are promising for near-term quantum computing platforms where measurement resources are constrained. By measuring a strategically chosen subset of operators and using a trained neural network, entanglement can be identified much more efficiently than through full state tomography, saving experimental time and classical post-processing resources.

Future work could explore several directions:

- Developing adaptive measurement strategies where the choice of the next measurement depends on previous outcomes, potentially reducing the required number of observables further.
- Incorporating noise models into the training process to make the classifier robust to experimental imperfections found in real quantum hardware.
- Extending the methodology to detect multipartite entanglement in systems with more than two qubits, where the resource cost of tomography scales even more unfavorably.

This work shows that machine learning offers a viable path towards resource-efficient quantum state characterization, helping to bridge the gap between theoretical concepts like entanglement and their practical verification in experiments.

ACKNOWLEDGMENT

This work was supported by the National Research Foundation of Korea (NRF) grant funded by the Korean government (MSIT) under RS-2025-00556064, and by the MSIT (Ministry of Science and ICT), Korea, under the ITRC (Information Technology Research Center) support program (IITP-2025-2021-0-02046) supervised by the IITP (Institute for Information & Communications Technology Planning & Evaluation) and by a grant from Kyung Hee University in 2023 (KHU-20233663).

REFERENCES

[1] M. A. Nielsen and I. L. Chuang, *Quantum Computation and Quantum Information: 10th Anniversary Edition*. Cambridge, UK: Cambridge University Press, 2010. (Placeholder for actual reference [1])

[2] J. Ureña, A. Sojo, J. Bermejo-Vega, and D. Manzano, "Entanglement detection with classical deep neural networks," *Scientific Reports*, vol. 14, no. 18109, 2024. Available: https://www.nature.com/articles/s41598-024-68213-0, doi: 10.1038/s41598-024-68213-0.

[3] N. Asif, U. Khalid, A. Khan, T. Q. Duong, and H. Shin, "Entanglement detection with artificial neural networks," *Scientific Reports*, vol. 13, no. 1562, 2023. Available: https://www.nature.com/articles/s41598-023-28745-3, doi: 10.1038/s41598-023-28745-3.

[4] Bonny, T., and A. Haq. "Emulation of high-performance correlation-based quantum clustering algorithm for two-dimensional data on FPGA." *Quantum Information Processing*, vol. 19, no. 179, 2020. https://doi.org/10.1007/s11128-020-02683-9

[5] UlHaq, A., and T. Bonny. "Cancer transcriptome analysis with RNA-seq using quantum k-means clustering algorithm." *Proceedings of the IEEE International Conference on Engineering Innovations in Healthcare*, 2020.

[6] W. K. Wootters, "Entanglement of Formation of an Arbitrary State of Two Qubits," *Phys. Rev. Lett.*, vol. 80, no. 10, pp. 2245–2248, Mar. 1998. (Placeholder for actual reference [2])